

Supporting Information

Water-Induced Phase Separation Enables Underwater Adhesive far exceeding Dry Adhesion

Pan Du^{a,b}, Yan Wang^{a,b} and Xianru He^{a,}*

Table of contents

- 1. Materials**
- 2. Charaterization of SSHU-adhesive**
- 3. Figures**
- 4. Supporting tables and movies**
- 5. References**

1. Materials

Acrylonitrile (AN), Butyl acrylate (BA), Anisole, Triethylene glycol dimethacrylate (TEGDMA), Benzoyl Peroxide (BPO), p-Tolyldiethanolamine, Methyl methacrylate (MMA), Methyl acrylate(MA), Hydroxypropyl methacrylate(HPMA), Hydroxyethyl acrylate(HEA) and Decane were purchased from Aladdin Chemical, China. 2,2'-Azobis(2-methylpropionitrile) (AIBN) from Cologne Chemical, Chengdu. Rhodamine 110 chloride was purchased from Shanghai yuanye Bio-Technology Co., Ltd. 1,1'-dioctadecyl-3,3,3',3'-tetramethylindocarbocyanine perchlorate was bought from Aladdin Chemical. Phosphotungstic acid solution (2 wt%) was from Shanghai Yien Chemical Technology Co., Ltd. Both AN and BA were purified from inhibitors by Al₂O₃ column. AIBN was recrystallized from Ethanol. PMMA, PVC, PTFE were purchased from KAIJING PLASTIC CO.,LTD. SS304, Al5052 were from YONGJIN CORPARATION, and Glass from Shahe anquan shiye Co., Ltd.

2. Charaterization of SSHU-adhesive

Fourier-transform IR (FT-IR) spectra for SSHU-adhesive and its component P(AN-co-BA) was characterized by Thermo Fisher Scientific Nicolet iS20. To testify crystallization of P(AN-co-BA), X-ray diffraction (XRD) measurements and Differential scanning calorimetry (DSC) were performed on Bruker D8 Advance diffractometer (Cu Ka radiation, $\lambda=1.504 \text{ \AA}$) and Mettler Toledo DSC823e under nitrogen atmosphere with heating and cooling rate of $5 \text{ }^\circ\text{C min}^{-1}$. 3D morphology, roughness and surface modulus was tested by Atomic force microscopy (Bruker Dimension ICON). Binding energy element on adhesive was measured by X-ray photoelectron spectroscope (XPS) (Thermo Scientific K-Alpha). Water droplet dispersion in polar monomer was observed by optical microscope (AMG EVOSFL). To further observe dispersion of water and monomer, dyed with Rhodamine 110 chloride and 1,1'-dioctadecyl-3,3,3',3'-tetramethylindocarbocyanine perchlorate with 10 nm/L respectively, confocal fluorescence microscopy (Leica STELLARIS 5) was conducted with excitation wavelength 488 nm, 561 nm and emission wavelength 520

nm, 565 nm respectively. To monitor phase separation of P(AN-co-BA) in water, as well as distribution of water dyed by Rhodamine 110 chloride with 10 nm/L, confocal fluorescence microscopy was also carried out by Leica STELLARIS 5. Wetting ability of adhesive on substrate was assessed by Dynamic contact angle (KRUSS DSA30S). Scanning Electron Microscopy (SEM) analysis was to observe microstructure of adhesive after lap shear tensile by ZEISS Sigma 300 with accelerating voltage of 3 kV. For high-resolution transmission electron microscopy (TEM) (FEI Talos F200X G2) observation, adhesive on PVC was immersed in Phosphotungstic acid solution with 2wt% for 15 hours, then surface adhesive layer with approximate 50 nanometers thick was detached by Focused Ion Beam sampling (FEI Scios 2 HiVac) after location by SEM associated with Energy Dispersive Spectroscopy (EDS).

3. Figures

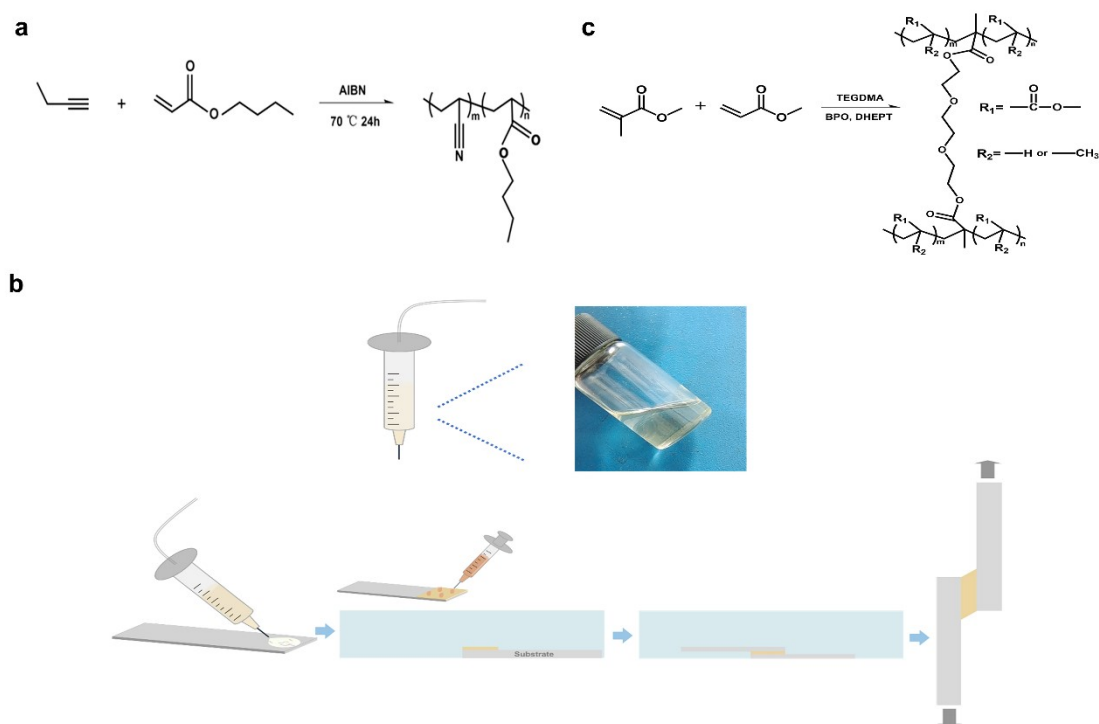


Figure S1. (a) Chemical reaction equation for P(AN-co-BA). (b) Schematic illustration of sample preparation for shear lap strength. (c) Chemical crosslinking reaction amid adhesive curing underwater.

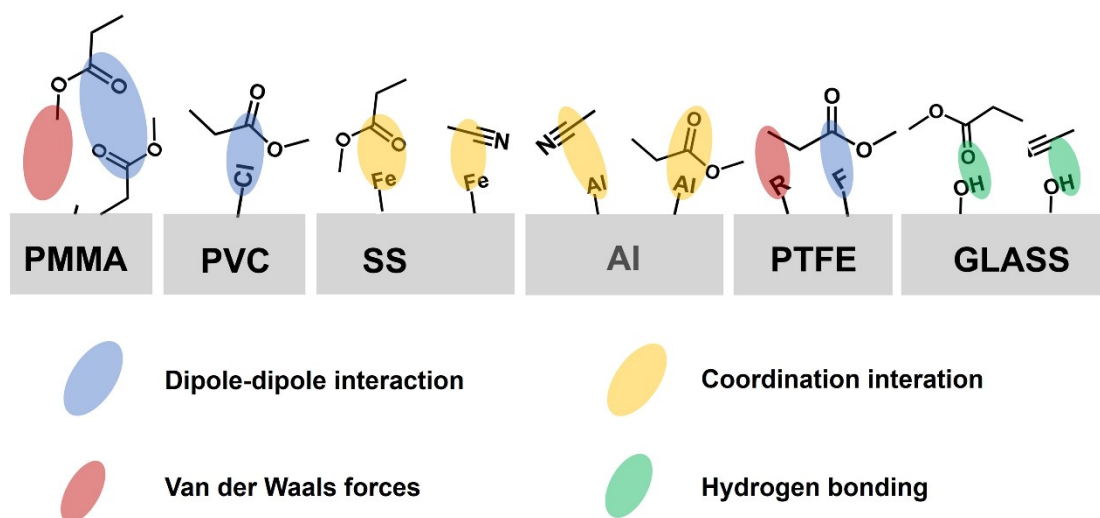


Figure S2. Interaction between adhesive and substrate.

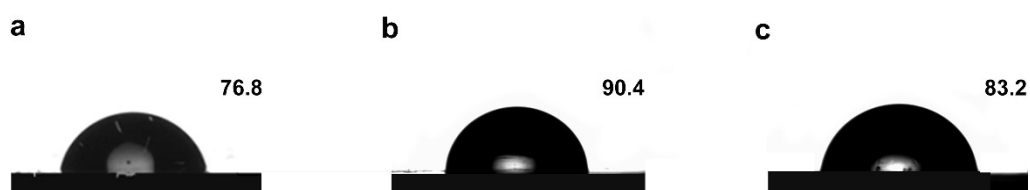


Figure S3. (a) Contact angle of water-air-PVC. (b) Contact angle of water-air-adhesive P(AN-co-BA)-P(MMA-co-HPMA) on PVC curing underwater. (c) Contact angle of water-air-adhesive P(AN-co-BA)-P(MMA-co-HPMA) on PVC curing in air.

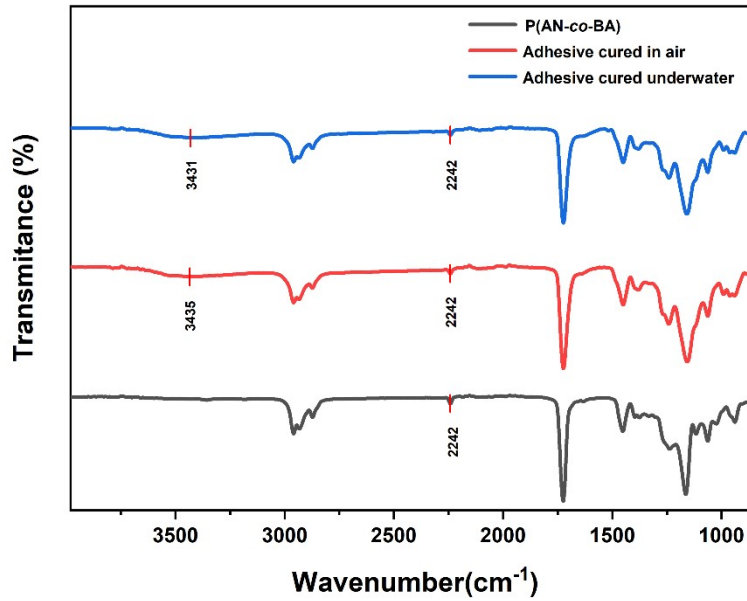


Figure S4. FT-IR spectra of P(AN-co-BA), adhesive P(AN-co-BA)-P(MMA-co-HPMA) cured in air, adhesive P(AN-co-BA)-P(MMA-co-HPMA) cured underwater. Compared to adhesive P(AN-co-BA)-P(MMA-co-HPMA) cured in air, peak donating -OH of adhesive cured underwater shifts to lower wavenumber, indicating that hydrogen bond formation between -OH due to aggregation of HPMA after phase separation of P(AN-co-BA).

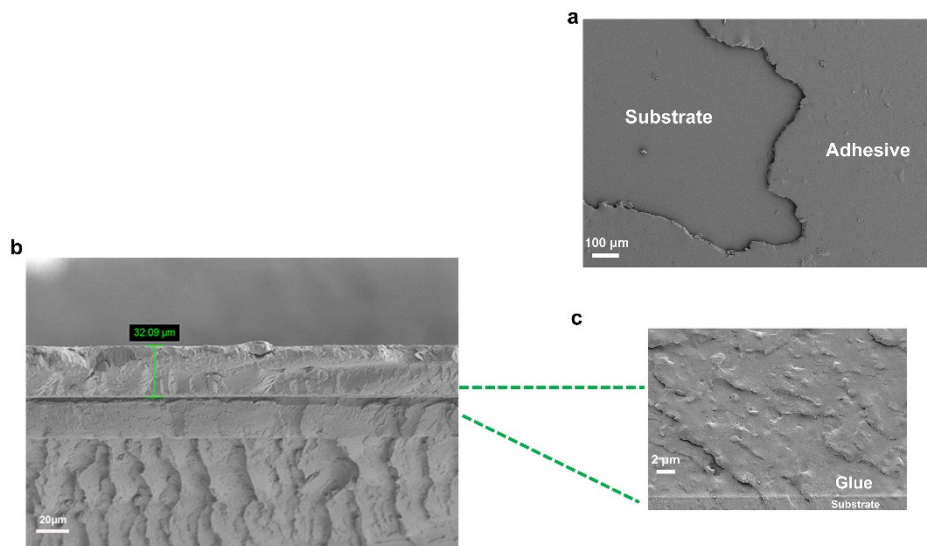


Figure S5. (a) Cohesive failure of underwater adhesive. (b) SEM image of adhesion layer with thickness of 32.09 μm . (c) SEM of cross-section of adhesive cured underwater showing distributed particle in bulk and close contact with PVC substrate.

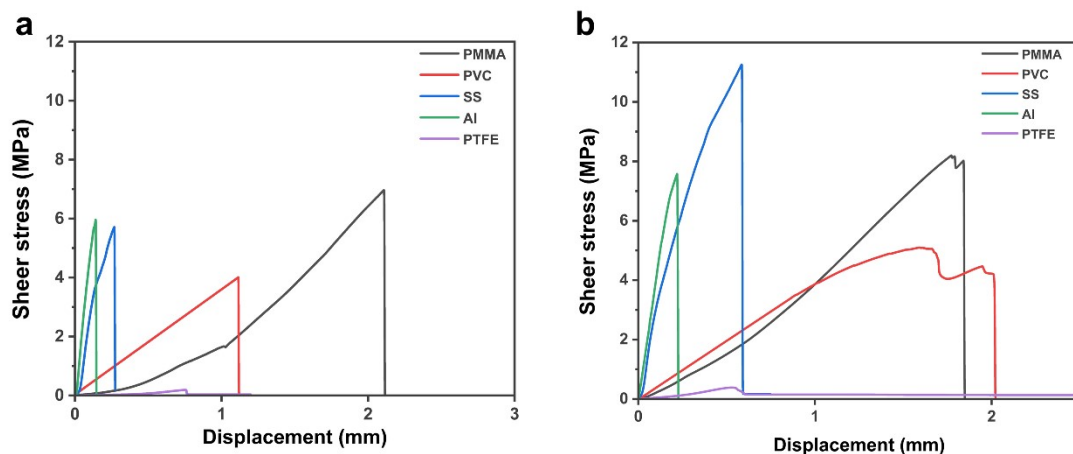


Figure S6. Lap shear strength test of adhesive with composition of P(AN-co-BA)₅₀-MMA/MA 91. (a) Shear stress-displacement curve of adhesive curing underwater. (b) Shear stress-displacement curve of adhesive curing in air.

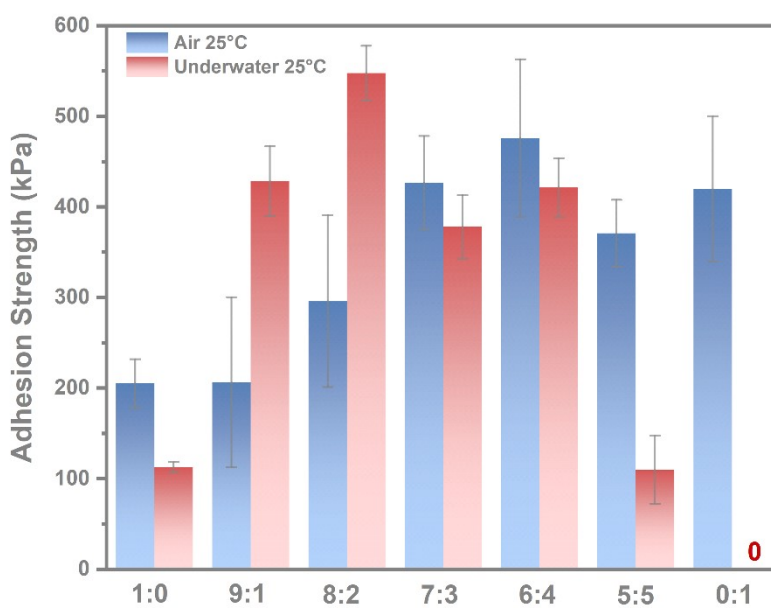


Figure S7. Lap shear adhesive strength on PTFE of SSHU-adhesive made up by P(AN-co-BA)₅₀ dissolved in various ratio of MMA and MA.

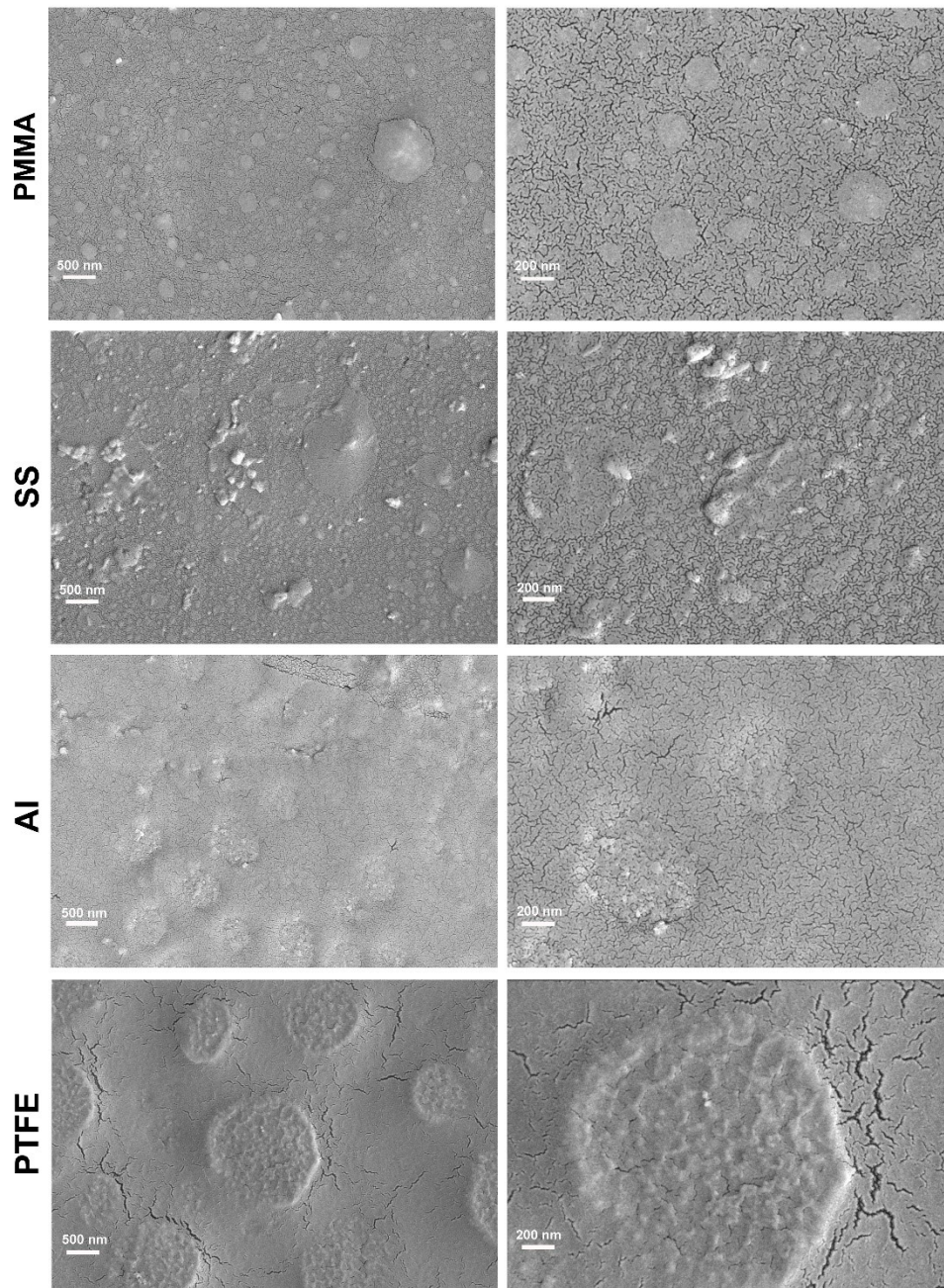


Figure S8. In SEM observation, surface structure of adhesive applied to different substrates underwater after shear lap strength test, showing distributed particles.

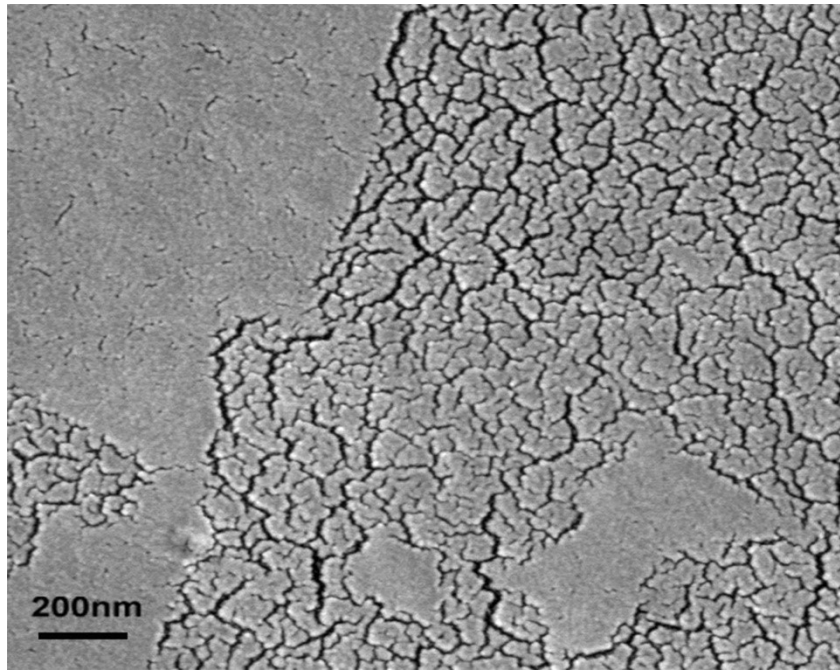
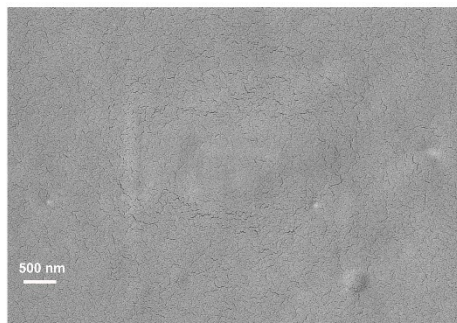
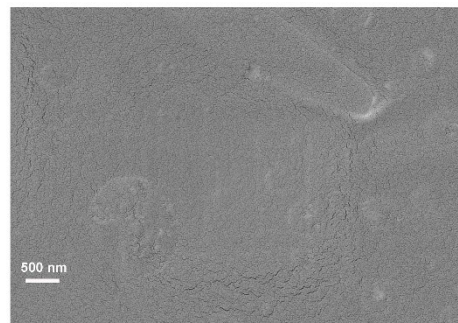


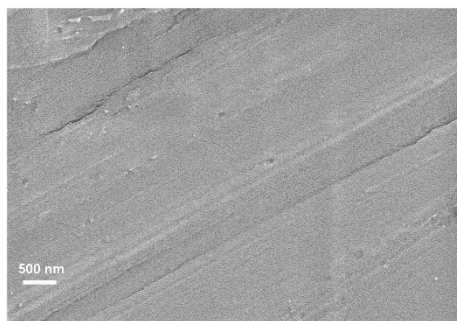
Figure S9. Surface structure of adhesive applied to PVC in air by SEM, showing no particle.



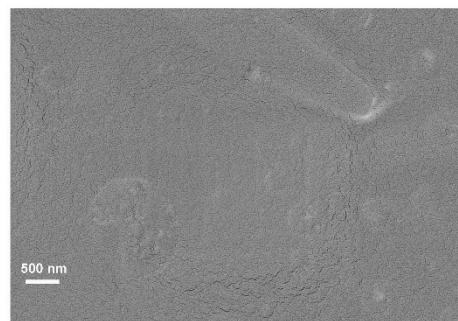
PMMA



SS



Al



PTFE

Figure S10. Surface structure of adhesive applied to different substrates in air by SEM, showing no particle.

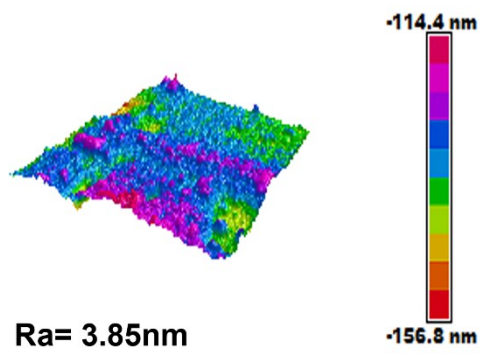


Figure S11. Roughness average value of PVC sheet acquired by atomic force microscopy (AFM).

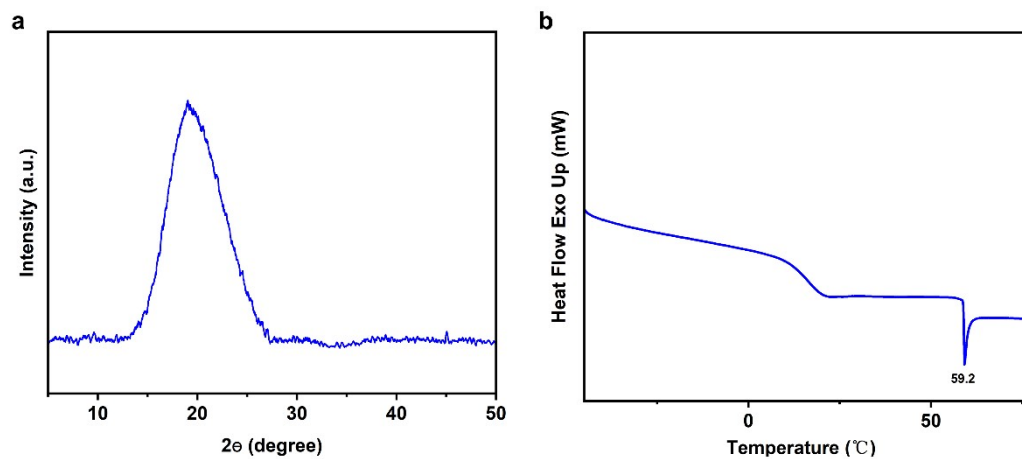


Figure S12. Crystallization characterization of P(AN-co-BA). (a) XRD profiles of P(AN-co-BA) film. (b) DSC of P(AN-co-BA) with T_g and melting temperature.

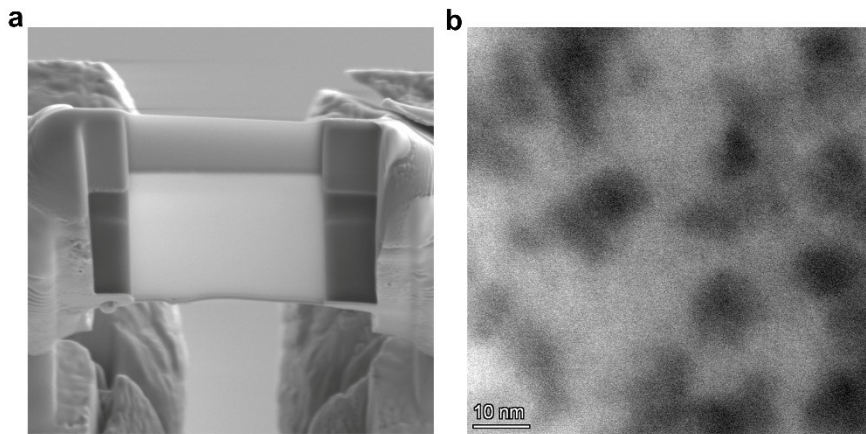


Figure S13. (a) Surface adhesive layer with approximate 50 nanometers thick was detached by Focused Ion Beam sampling (FEI Scios 2 HiVac) after location by SEM associated with Energy Dispersive Spectroscopy (EDS). (b) Phase separation of P(AN-co-BA) dyed by phosphotungstic acid solution with approximate 10 nm by TEM.

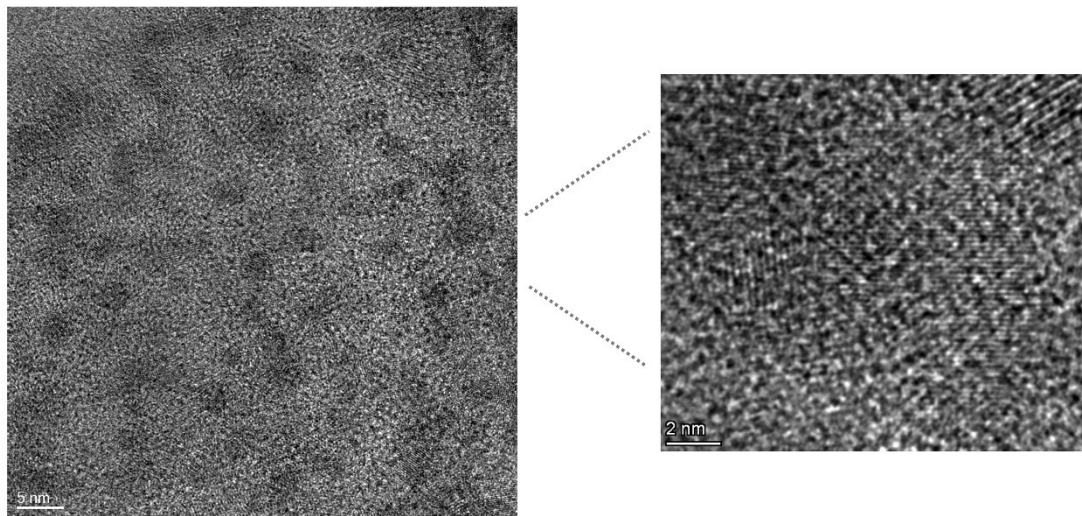


Figure S14. Interference fringes responsible for crystallization of P(AN-co-BA) in nanoparticle observed by TEM.

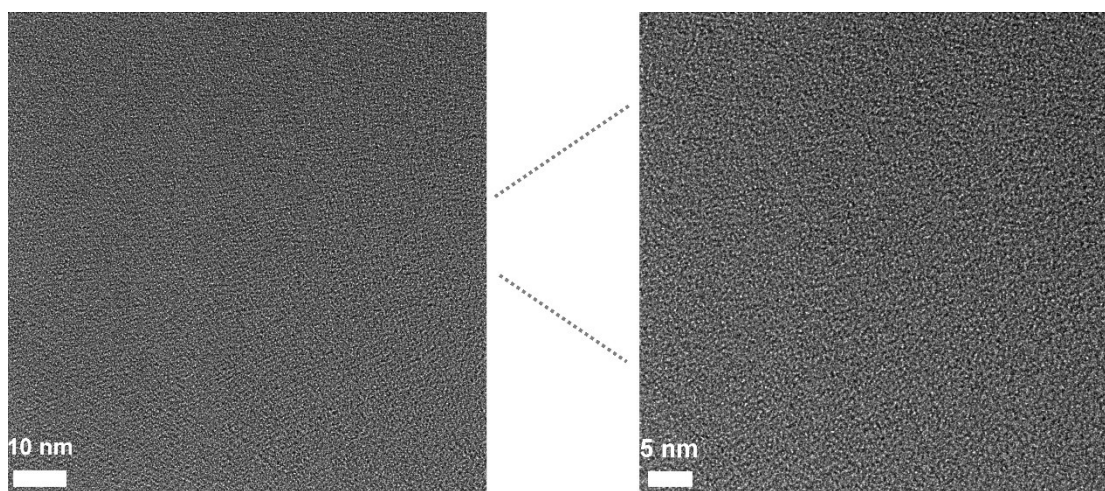


Figure S15. No interference fringes observed by TEM indicating no crystallization of P(AN-co-BA).

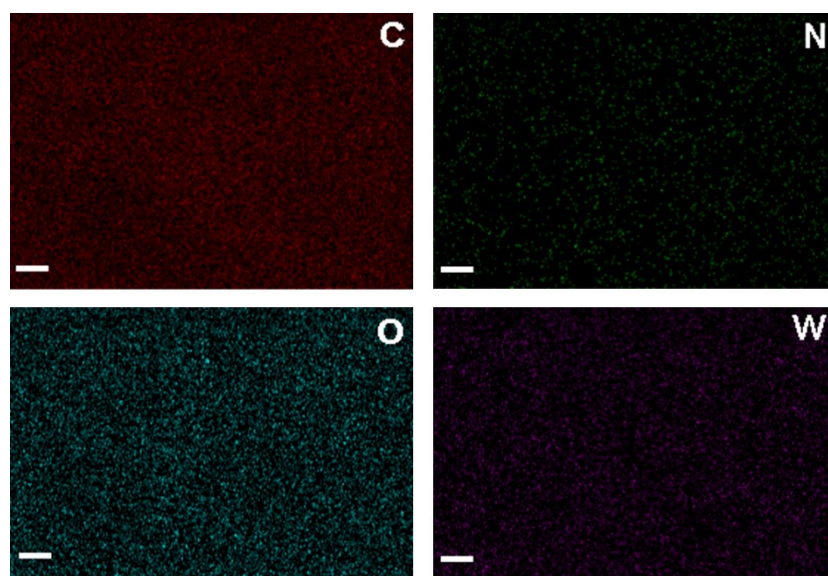


Figure S16. After 15-hour immersion in Phosphotungstic acid solution with 2wt%, EDS test for atomic distribution of adhesive curing in air, showing that W was successfully dyed on acrylonitrile (AN) structural unit.



Figure S17. Lap joint area with adhesive curing underwater for 5 minutes can bear 50 Kg weight.

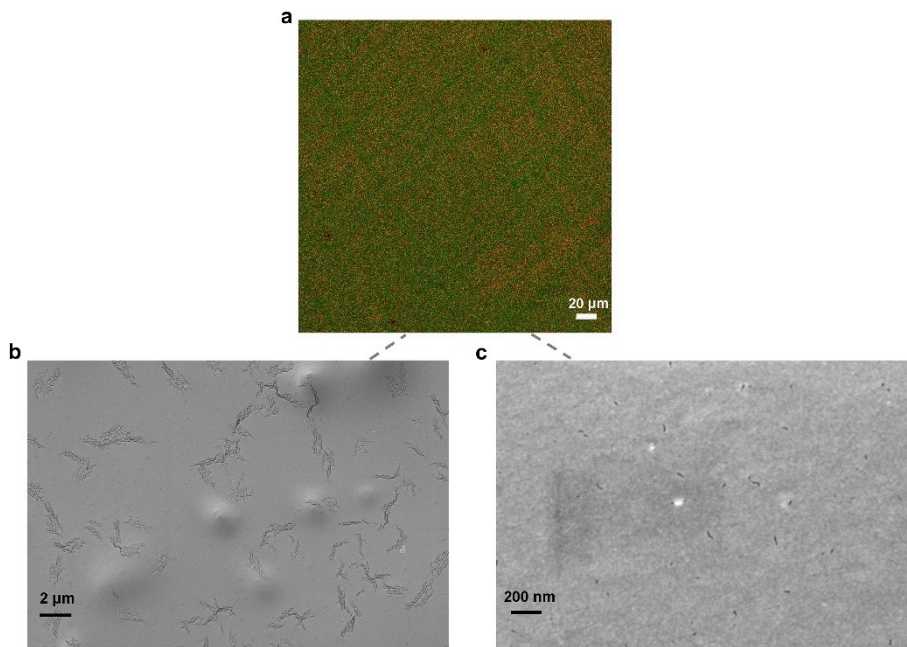


Figure S18. (a) Degree of miscibility of dyed water with dyed monomer by confocal fluorescence microscopy with ratio of MMA/MA 0/10. Green fluorescence represents water dyed with Rhodamine 110 chloride, while red fluorescence represents MA dyed

with 1,1'-dioctadecyl-3,3,3',3' tetramethylindocarbocyanine perchlorate (b-c) Surface microstructure of underwater adhesive comprised of P(AN-co-BA)-PMA. Barely nanoparticle formed underwater due to higher solubility of MA compared to MMA, resulting in less improvement for adhesive strength.

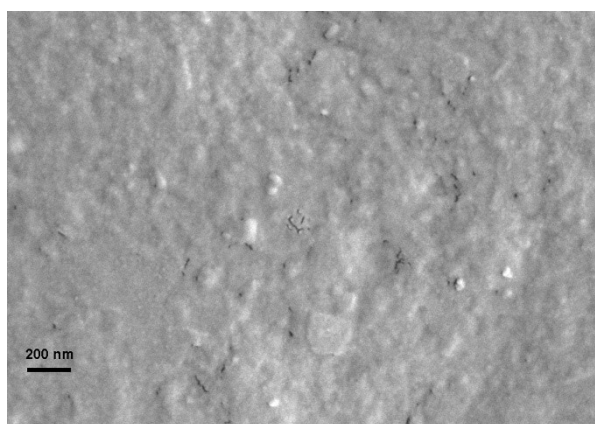


Figure S19. Surface microstructure of underwater adhesive on PVC comprised of P(AN-co-BA)₅₅-PMMA, with mole percent of AN is 45% in P(AN-co-BA).

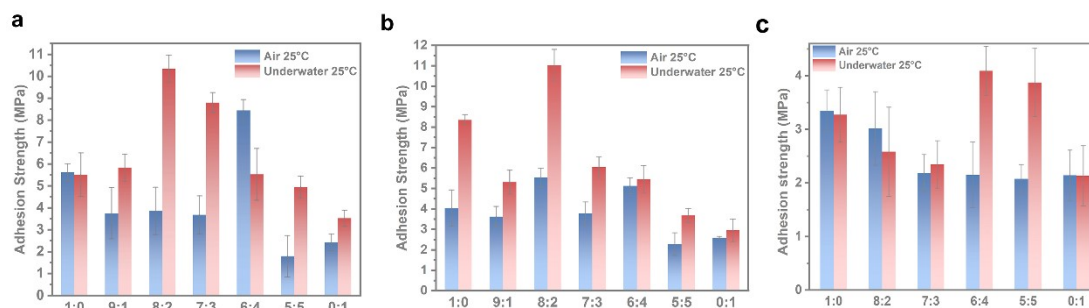


Figure S20. Lap shear adhesion to PVC of SSHU-adhesive prepared by P(AN-co-BA)₅₅, P(AN-co-BA)₅₀, P(AN-co-BA)₄₀ dissolved in various ratio of MMA and MA.

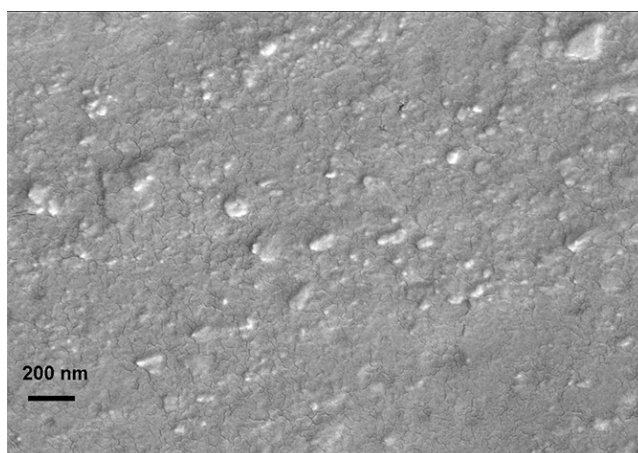


Figure S21. Surface microstructure of underwater adhesion to PVC comprised of $P(\text{AN-co-BA})_{40}$ -PMMA.

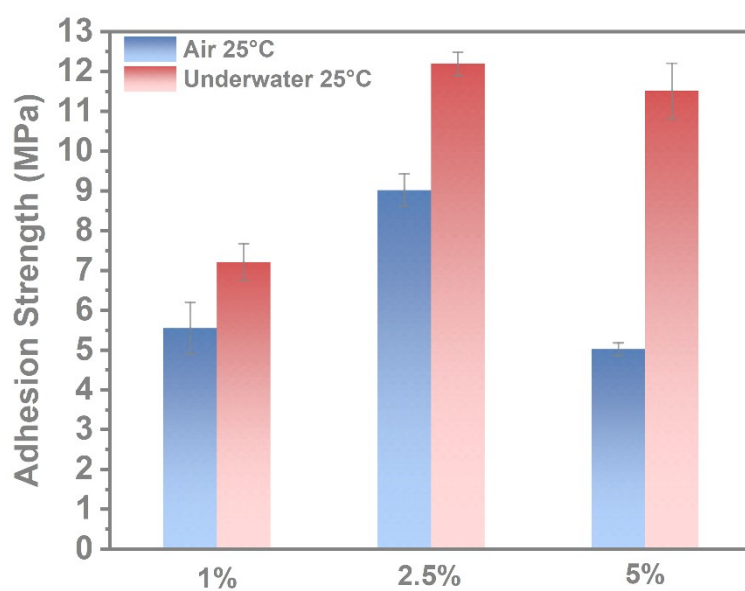


Figure S22. Lap shear adhesive adhesion to PVC of SSHU-adhesive with various mole content of crosslinking agent accounting for monomer.

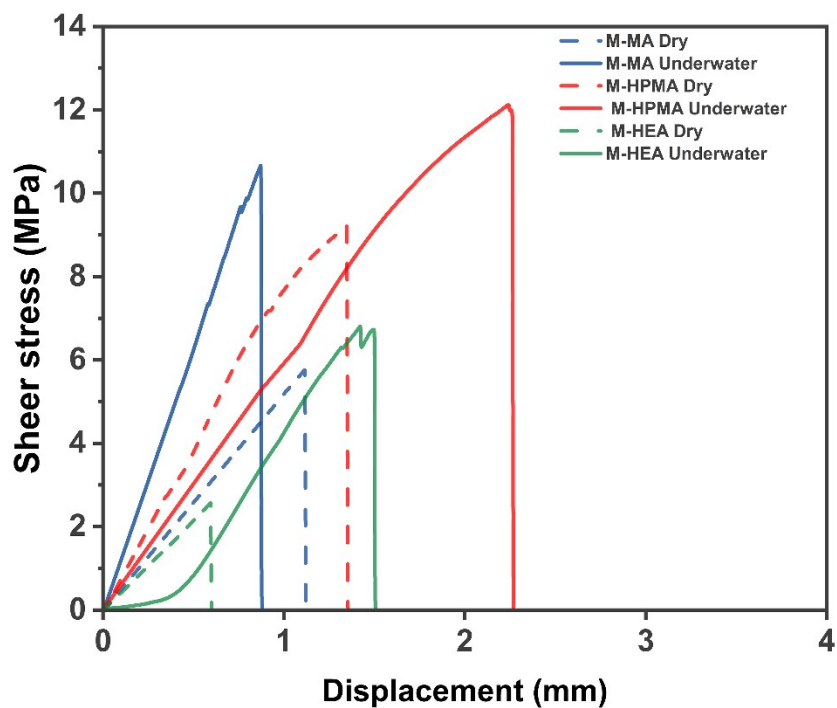


Figure S23. Lap shear strength test of adhesive with composition of P(AN-co-BA)₅₀-MMA/MA 82, P(AN-co-BA)₅₀-MMA/HPMA 82 and P(AN-co-BA)₅₀-MMA/HEA 82 respectively.

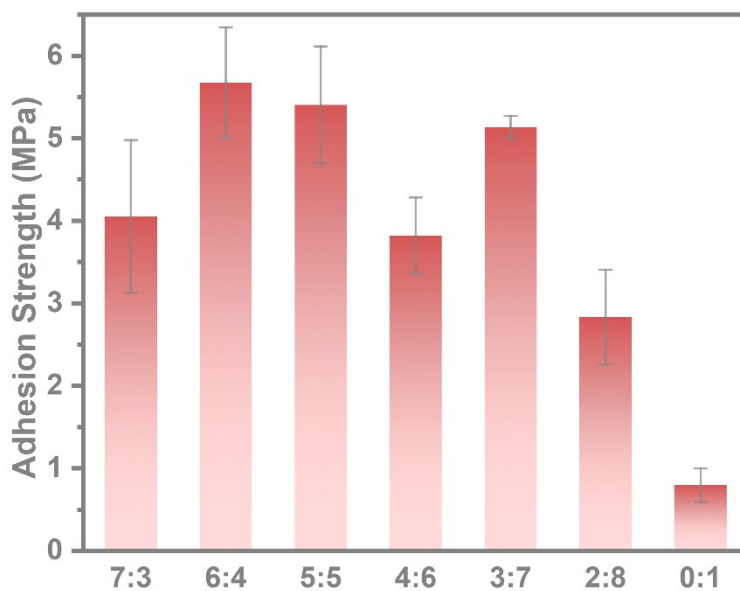


Figure S24. Lap shear adhesion to glass of SSHU-adhesive with various ratio of HPMA and MA.

4. Supporting tables and movies

Table S1. Atomic content of adhesive P(AN-*co*-BA)-P(MMA-*co*-MA) on PVC curing in air by EDS.

Element	At%
C	78.32
N	3.15
O	18.16
W	0.37

Table S2. Atomic content in adhesive P(AN-*co*-BA)-P(MMA-*co*-HPMA) according to broad scan of XPS spectra.

Adhesive	Atomic content (%)		
	C	N	O
underwater	75.78	5.59	18.63
air	75.34	4.04	20.62

Table S3. Underwater adhesion performance comparison of SSHU-adhesive and lately reported adhesive on PMMA and SS

Adhesive	Underwater lap shear strength on PMMA/SS(Mpa)	Curing time	Curing condition	Water resistance
SSHU-adhesive	9.26/10.97	5min	In-situ polymerization	180 days
AFBA[1]	0.26/0.49	24 h	Solvent exchange	30 days

POC[2]	0.76/2.02	10 min	Solvent exchange	N/A
Ionogel[3]	3.1/4.58	2 h	ionogel dynamic crosslinking	180 days
SLU-adhesive[4]	0.745/ N/A	12.5 h	isocyanate group reaction with water	N/A
PVP-AA adhesive[5]	4.6/ N/A	10 s	In-situ photocuring	30 days
Poly(catechol-styrene)[6]	N/A /0.1	24 h	Solvent exchange	N/A
PUP-PPG-DBHP[7]	N/A /1	30 s	isocyanate group reaction with water	—
P4-AS-PAA[8]	0.36/ N/A	20 min	4-AS Spontaneously Polymerized	180 days
P1[9]	0.618/3.237	24 h	Hot meltingP1	24 hour

Movie S1

Spontaneously spreading of SSHU-adhesive on substrate in water

Movie S2

Lap joint area can bear 50 Kg weight after 5-minute curing

References

- [1] F. Li, W. Gu, S. Gong, W. Zhou, S.Q. Shi, Q. Gao, Z. Fang, J. Li, Design of amphiphilic-function-aiding biopolymer adhesives for strong and durable underwater adhesion via a simple solvent-exchange approach, *Chem Eng J* 469 (2023) 143793.
- [2] Y.H. Li, Z.Y. Liu, T.C. Wang, M.L. Wang, H.R. Yao, F. Gao, J. Cheng, J.Y. Zhang, Barnacle-inspired amphipathic high strength adhesives under-water/oil, *Chem Eng J* 498 (2024).
- [3] S. Wang, R. Ou, J. Li, K. Jin, L. Yu, P. Murto, Z. Wang, X. Xu, Deformation-Resistant Underwater Adhesion in a Wide Salinity Range, *Small* 20(44) (2024) 2403350.
- [4] C. Qin, Y. Ma, Z. Zhang, Y. Du, S. Duan, S. Ma, X. Pei, B. Yu, M. Cai, X. He, F. Zhou, Water-assisted strong underwater adhesion via interfacial water removal and self-adaptive gelation, *Proc Natl Acad Sci U S A* 120(31) (2023) e2301364120.
- [5] Y.S. Zhou, C. Zhang, S.W. Gao, B.P. Zhang, J. Sun, J.J. Kai, B. Wang, Z.K. Wang, Instant and Strong Underwater Adhesion by Coupling Hygroscopicity and In Situ Photocuring, *Chem Mater* 33(22) (2021) 8822-8830.
- [6] M.A. North, C.A. Del Grosso, J.J. Wilker, High Strength Underwater Bonding with Polymer Mimics of Mussel Adhesive Proteins, *Acs Appl Mater Inter* 9(8) (2017) 7866-7872.
- [7] G.Z. Xia, M. Lin, Y. Jiayu, H. Jinkang, L. Bowen, Y.B. Mu, X.B. Wan, Solvent-Free Mussel-Inspired Adhesive with Rapid Underwater Curing Capability, *Adv Mater Interfaces* 8(21) (2021).
- [8] C.Y. Cui, R.H. Gu, T.L. Wu, Z.Y. Yuan, C.C. Fan, Y. Yao, Z.Y. Xu, B. Liu, J.Y. Huang, W.G. Liu, Zwitterion-Initiated Spontaneously Polymerized Super Adhesive Showing Real-Time Deployable and Long-Term High-Strength Adhesion against Various Harsh Environments, *Advanced Functional Materials* 32(4) (2022).
- [9] C.Y. Sun, J.B. Luo, T.X. Jia, C.Y. Hou, Y.G. Li, Q.H. Zhang, H.Z. Wang, Water-resistant and underwater adhesive ion-conducting gel for motion-robust bioelectric monitoring, *Chem Eng J* 431 (2022).